

We are IntechOpen, the world's leading publisher of Open Access books Built by scientists, for scientists

6,900

Open access books available

186,000

International authors and editors

200M

Downloads

Our authors are among the

154

Countries delivered to

TOP 1%

most cited scientists

12.2%

Contributors from top 500 universities



WEB OF SCIENCE™

Selection of our books indexed in the Book Citation Index
in Web of Science™ Core Collection (BKCI)

Interested in publishing with us?
Contact book.department@intechopen.com

Numbers displayed above are based on latest data collected.
For more information visit www.intechopen.com



Validation and Application of SMAP SSS Observation in Chinese Coastal Seas

Qiong Wu, Xiaochun Wang, Xianqiang He and
Wenhao Liang

Additional information is available at the end of the chapter

<http://dx.doi.org/10.5772/intechopen.80318>

Abstract

Using sea surface salinity (SSS) from the Soil Moisture Active Passive (SMAP) mission from September 2015 to August 2016, the spatial distribution and seasonal variation in SSS in the Chinese coastal seas were investigated. First, in situ salinity observation over Chinese East Sea was used to validate SMAP observation. Then, the SSS signature of the Yangtze River fresh water was analyzed using SMAP data and the river discharge data. The SSS around the Yangtze River estuary in the Chinese East Sea, the Bohai Sea and the Yellow Sea is significantly lower than that of the open ocean. The SSS of Chinese coastal seas shows significant seasonal variation, and the seasonal variation in the adjacent waters of the Yangtze River estuary is the most obvious, followed by that of the Pearl River estuary. The minimum value of SSS appears in summer while maximum in winter. The root-mean-squared difference of daily SSS between SMAP observation and in situ observation is around 3 psu in both summer and winter, which is much lower than the annual range of SSS variation. The path of fresh water from SMAP and in situ observation is consistent during summer time.

Keywords: SMAP, CTD (conductance, temperature and depth), SSS (sea surface salinity), Yangtze River estuary

1. Introduction

Sea surface salinity (SSS) is one of the most important variables in describing the basic state of the ocean and can also be considered a proxy for the impact of the hydrologic cycle or the flux of freshwater across the air-sea interface [1]. The areas of low SSS tend to be regions where

precipitation is a dominant process with a net transport of freshwater from the atmosphere to the ocean [2]. The observation of SSS can enhance the understanding of the global water cycle. SSS is also an important tracer of the water mass.

Field observation and satellite remote sensing are two main methods to obtain SSS data (e.g., [3–4]). Field observation is extensively used in scientific research and operational monitoring of the ocean. Subrahmanyam et al. [5] used temperature and salinity profile data from Argo floats to investigate the seasonal and inter annual variations of SSS over the equatorial east India Ocean. Liu et al. [6] analyzed the influence of the wind on the extension of the Yangtze River freshwater plume northeast by using the salinity data from two zonal sections near Jeju Island. Although salinity data can be obtained from in situ observations, it cannot describe the changes of salinity at fine spatial scales due to the sparse distribution of in situ measurements. The maturity of the SSS satellite observation method provides a new way for the study of SSS. In recent years, several satellites have been launched, such as SMOS, AQUARIUS and SMAP for observing salinity. SMOS is the first SSS satellite mission launched by the European Space Agency in 2009 (e.g., [7–8]). AQUARIUS is a passive/active L band microwave instrument jointly launched by NASA and Argentina Space Agency in 2011 to observe the SSS (e.g., [9–11]). The Soil Moisture Active Passive (SMAP) satellite is the first satellite of the United States Space Agency (NASA) to detect soil moisture, which was launched on 31 January, 2015. The L band radar and radiometer on the SMAP satellite can also observe SSS. In order to achieve larger coverage on the ground and ocean, the antenna of SMAP rotates at a speed of 14.6 cycles per minute. The orbit of the SMAP is combined with the rotation of the antenna, forming a 1000 km wide observation stripe. This large area coverage makes SMAP complete the measurement of the Earth surface every 2–3 days (e.g., [12–15]). The SSS from SMAP can also show the freshwater plume of many large rivers, such as the Amazon River, Niger River, Ganges River, Nuijiang and the Mississippi River [15]. In addition, the validation of SMAP observation was conducted for various regions. For example, Fournier et al. [16] showed a general agreement of SMAP SSS with in situ SSS over the Gulf of Mexico.

SSS satellite missions provide new opportunity to study SSS variation and their potential applications in terms of ocean monitoring and forecasting need to be explored, especially in coastal regions where the riverine freshwater discharge plays a significant role in oceanic processes and in situ salinity observation is often sparse in space. In present research, the SSS observation from SMAP mission is used to study SSS variation in Chinese coastal seas. Section 2 presents the data we used. Section 3 validates SMAP observation using in situ observation and analyzes SSS variability on seasonal and sub-seasonal time scales. Section 4 summarizes our results.

2. Data and methodology

The SSS product is obtained from NASA SMAP mission. A gridded product by blending original observation from 7 days is used in our analysis, which has a spatial resolution of 0.25 and a temporal resolution of 1 day. We used the gridded product from September 1, 2015 to August 31, 2016.

The in situ salinity measurements are from “Rongjiang No.1” research vessel. The field campaigns include a winter one from December 20 to 30, 2015 and a summer one from August 3 to 13, 2016. The sea-bird SBE conductivity, temperature, and depth (CTD) was used for all measurements. For each station, the CTD instrument was put in the water for 3–5 min and descends with a speed of 1 m/s. The procedure was repeated 1–2 times to get measurements. In our analysis, we found there are some spurious measurements and our quality control procedure includes two steps. The first step is to remove all the data that have pressure less than 0. The second step is to remove all data that are outside the three standard deviations of the mean.

The Yangtze River Datong hydrological station is located in the Meilong town of Chizhou, Anhui province. The station was built in the early twentieth century and is the upper boundary of the ocean tidal influence. This station has long-term observation data in the lower reaches of the Yangtze River basin. For the discharge data, we also selected data from September 2015 to August 2016.

3. Results

3.1. Validation

The daily gridded SSS observation from SMAP was first validated against in situ observation from two field campaigns around Yangtze River estuary. **Figure 1** shows the comparison of daily SSS from SMAP mission and in situ CTD observation for the winter of 2015 (**Figure 1a**), and summer of 2016 (**Figure 1b**). During the winter of 2015, the bias between in situ SSS and SMAP SSS observation is -1.36 psu, with SMAP mission overestimating SSS. The root mean square difference (RMSD) of the in situ and SMAP SSS observation is 3.15 psu. During the summer of 2016, the RMSD of in situ and SMAP SSS observation is 3.02 psu, with a bias of 0.47 psu. It is interesting to note that SMAP mission tends to overestimate SSS around Yangtze River estuary.

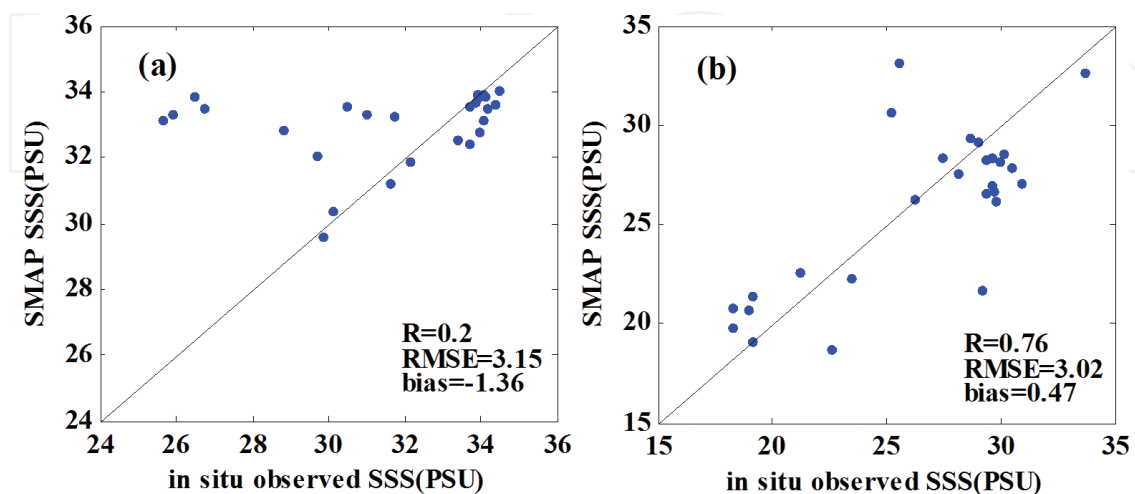


Figure 1. Comparison of daily SSS from SMAP mission and in situ CTD observation for (a) the winter of 2015 and (b) the summer of 2016. The unit for SSS is psu.

Though there is large bias of SMAP SSS observation during the winter of 2015, it is encouraging to note the similarity between SSS spatial distribution from SMAP (**Figure 2a**) and in situ measurement (**Figure 2b**). For instance, gradual increase of SSS from around 29–31 psu along 32°N is visible in both SMAP and in situ SSS observation. **Figure 2c** and **d** presents the distribution of SMAP and in situ CTD observation for the summer of 2016. The major feature in both SMAP and in situ SSS observation is the northeastward extension of Yangtze River freshwater plume, similar to the observations of Kim et al. [17] and Xuan et al. [18].

Though the errors in SMAP SSS observation are as large as 3 psu, it is encouraging to note that the SMAP SSS observation has great potential to monitor the spreading of freshwater plume from the Yangtze River.

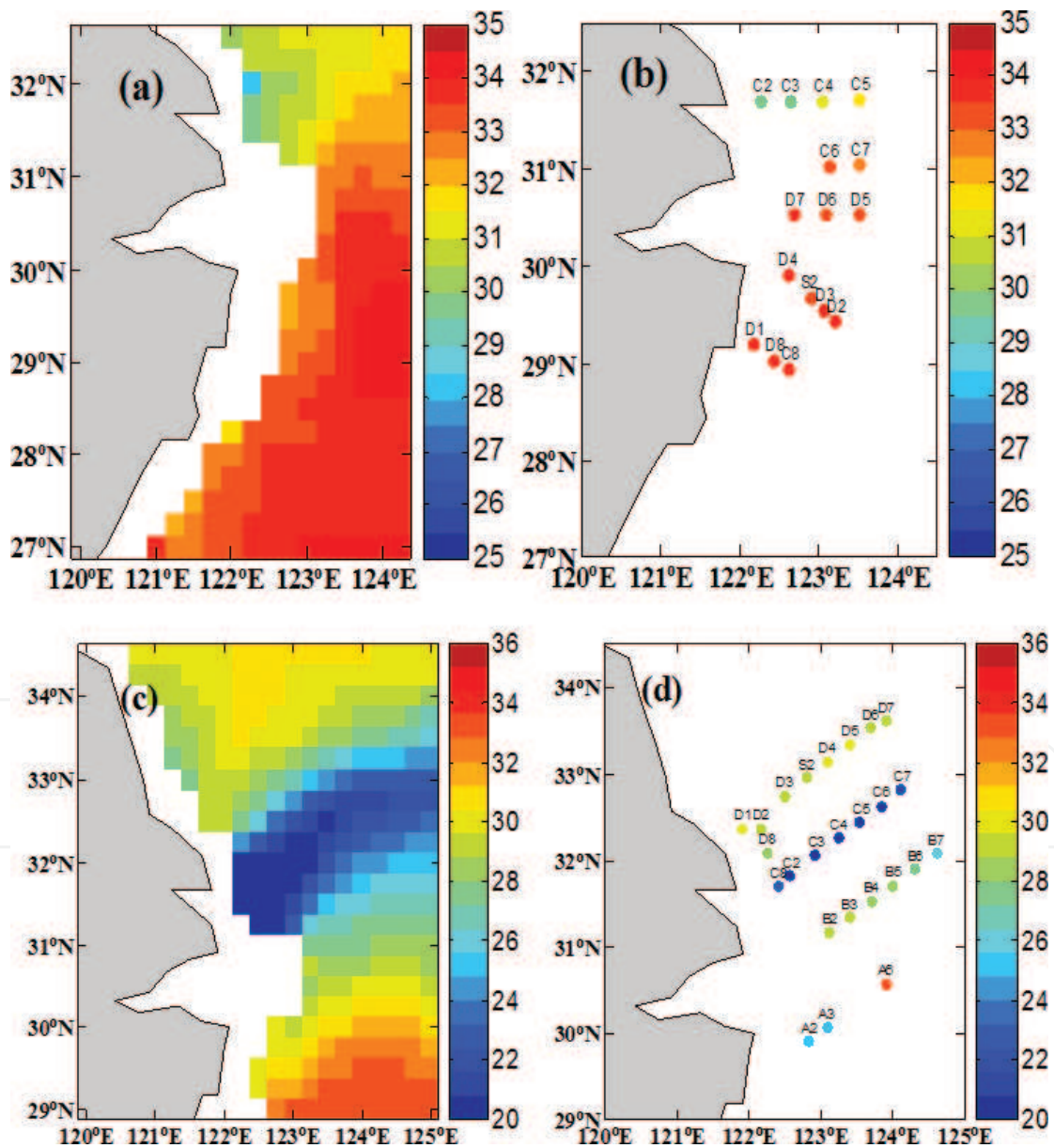


Figure 2. (a) SSS of SMAP from December 20 to 30, 2015; (b) SSS of in situ CTD observation from December 20 to 30, 2015; (c) SSS of SMAP from August 3 to 13, 2016 and (d) SSS of in situ CTD observation from August 3 to 13, 2016. The unit for SSS is psu.

3.2. Mean and range of SSS

Because of the sparseness of in situ observations, the fine spatial structure of SSS is poorly known over most coastal areas of China. However, the SMAP data (**Figure 3a**) show the spatial distribution of annual averaged SSS in different coastal areas of China. Due to the influence of discharge, the annual averaged SSS over Bohai Sea, Yellow Sea, and Yangtze River estuary are lower than other regions. The minimum value of SSS is about 25 psu around the Yangtze River estuary. The averaged SSS over South China Sea (SCS) is 33–34 psu, significantly higher than that of the Yellow Sea, Bohai Sea and Yangtze River estuary. However, the SSS over the SCS is lower than that of the Pacific Ocean. As seen from **Figure 3a**, the SSS gradient is large between the west and east side of the Luzon strait. Another feature is that the SSS is significantly decreased from the near coastal region to the outer sea.

In order to further illustrate the variability of SSS over the Chinese coastal regions, we calculated the differences of the maximum and the minimum values of SSS at each grid point (**Figure 3b**). The range of SSS changes is about 16 psu during 1 year. The Yangtze River estuary is associated with the large values while the amplitude of SSS decreases from the estuary to the outer sea. The influence of the Yangtze River is obvious in the spatial distribution of SSS range, with a belt of large SSS range extending northeastward from the Yangtze River estuary to Jeju Island.

3.3. Seasonal variation

The SSS of Chinese coastal seas experiences large seasonal variability. In **Figure 4a–d**, the low value SSS region over the Chinese coastal seas gradually retreats to the Bohai Sea from September 2015 to December 2015 and gradually invades the coastal regions from January 2016 to July 2016 (**Figure 4e–k**). The SSS reaches the minimum in July 2016 (**Figure 4k**), mainly due to the increasing precipitation over the Yangtze River basin from winter to summer. The Pearl River, which is the largest river in South China, also causes large SSS variability in coastal region. The SSS varies from 32 to 33 psu over Pearl River estuary from September 2015 to October 2015 (**Figure 4a, b**), and the SSS value decreases gradually from April 2016 to July 2016 (**Figure 4h–k**).

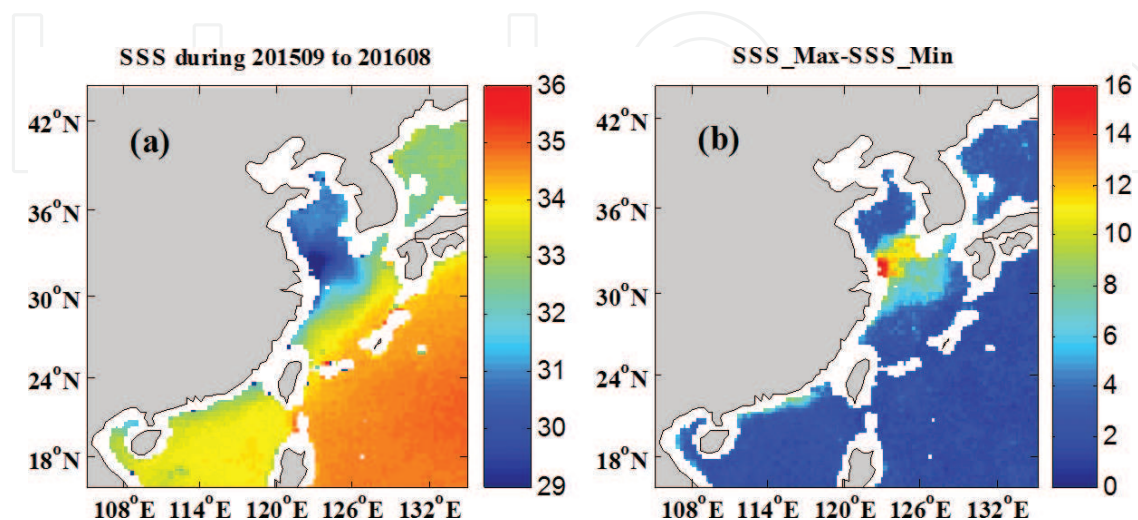


Figure 3. (a) Mean SMAP SSS from September 2015 to August 2016 in Chinese coastal seas. (b) The difference of maximum and minimum SSS. The unit for SSS is psu.

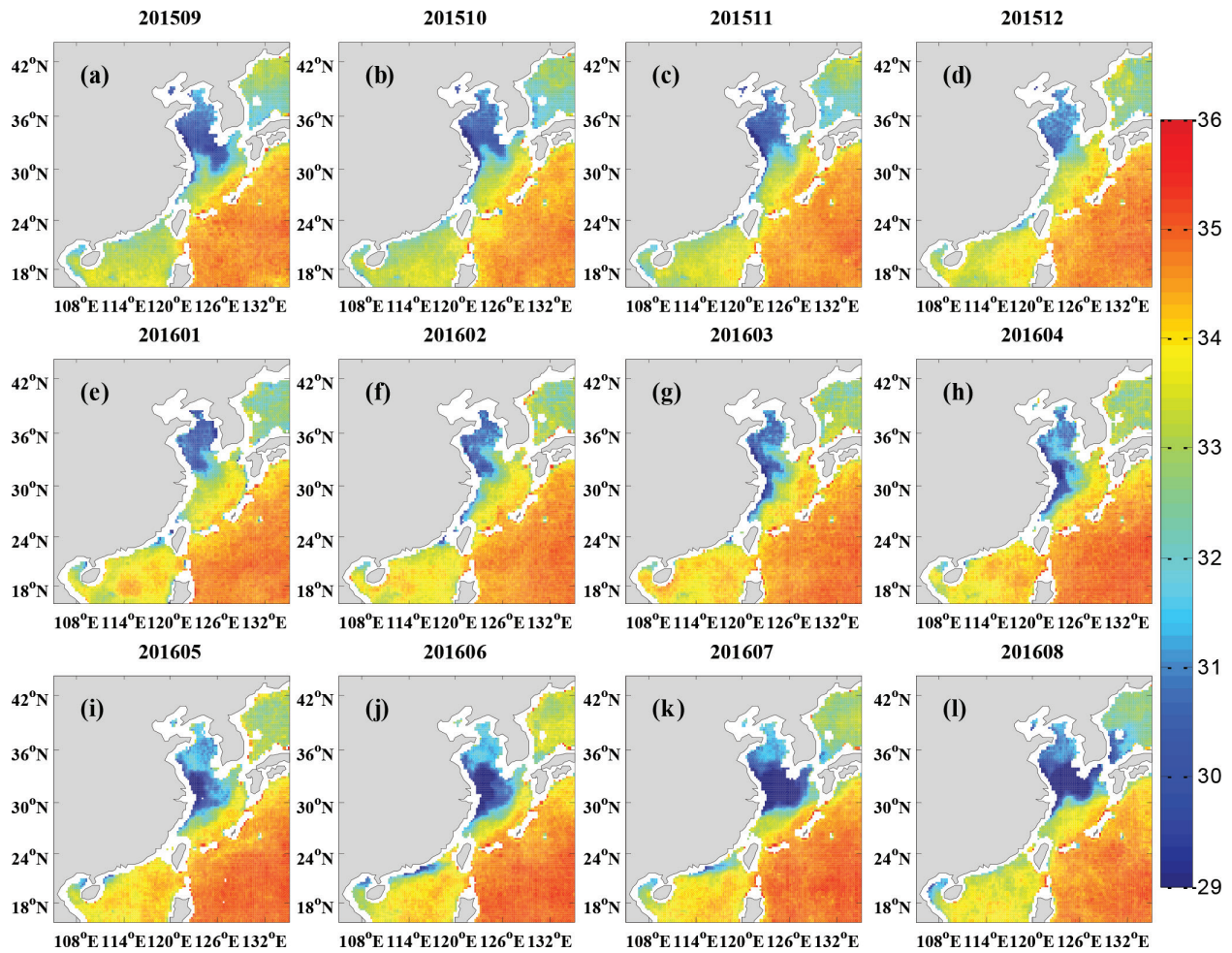


Figure 4. (a-l) Monthly SSS from September 2015 to August 2016 of Chinese coastal seas. The month is shown at the top part of each figure. The unit for SSS is psu.

Generally, the SSS of the Yangtze River estuary and the Pearl River estuary are relatively higher in winter and lower in summer, which reflects that the SSS variation in Chinese coastal seas is influenced by the precipitation and freshwater discharge.

To analyze the relationship of SSS change and hydrological cycle, the mean SSS from 32°N to 33°N, 122°E to 124°E is used as an index to represent SSS in the Yangtze River estuary. **Figure 5** presents the time evolution of SSS in the Yangtze River estuary and the Yangtze River discharge at Datong hydrological station.

The SSS of the Yangtze River estuary is around 31 psu from September 2015 to February 2016. At this time, the value of discharge is maintained from 2×10^4 to 3×10^4 m³/s. When the discharge increased gradually from February 2016 to July 2016, reaching a peak value of 7×10^4 m³/s in July of 2016, the SSS of the Yangtze River estuary fluctuated downward and the SSS value reached the minimum value of 24 psu in July of 2016. After July of 2016, the SSS increased rapidly following the decreasing of the discharge.

Overall, the time evolution of the mean SSS and discharge in Yangtze River estuary is opposite. Large discharge value corresponds to the low salinity, and the small discharge corresponds to

the high salinity. The correlation coefficient between them is -0.91 , which is significant at 99% confidence level. The above mentioned analysis indicates the potential of using SSS observation to infer the change of discharge for remote areas where the discharge observation is not available.

From **Figure 4a–l**, we can see that besides the Yangtze River estuary, SSS also shows a clear seasonal variation in the Pearl River estuary, but its variation is smaller than that in the Yangtze River estuary.

Rainy season usually appears in South China from April to May every year and ends around October. **Figure 6a** shows the time series of discharge from the Pearl River [19]. The discharge of the Pearl River is high in spring and in summer. The amount of discharge of Pearl River from April to September accounted for 79% of the total discharge of entire year while it is relatively small in winter, resulting in the seasonal variation of SSS. **Figure 6b–g** shows the evolution of SSS every 2 months from September 2015 to July 2016 over Pearl River estuary. It is obvious that the SSS over Pearl River estuary reaches the maximum in winter and the minimum in summer. The SSS in the coastal areas is lower than that of the outer sea.

3.4. Path of Yangtze River freshwater

Because of its high spatial and temporal resolution, SMAP observation can depict the diffusion and advection path of freshwater plume in the Yangtze River estuary very well. We can see that the Yangtze River plume spreads from near coastal region to the outer sea. The most obvious feature is that there is a clear trend of spreading to the northeast from May to July in 2016. By August, the trend of spreading to the northeast has weakened (**Figure 4**). In order to analyze the spreading of Yangtze River freshwater in summer, we showed the SSS distribution map of 15th and 30th of May, June, July in 2016 (**Figure 7a–f**). It can be seen that since May, the areas affected by Yangtze River freshwater become larger increasingly and the area of low salinity extends northeastward gradually. During the winter, there is a completely different diffusion path for the Yangtze River

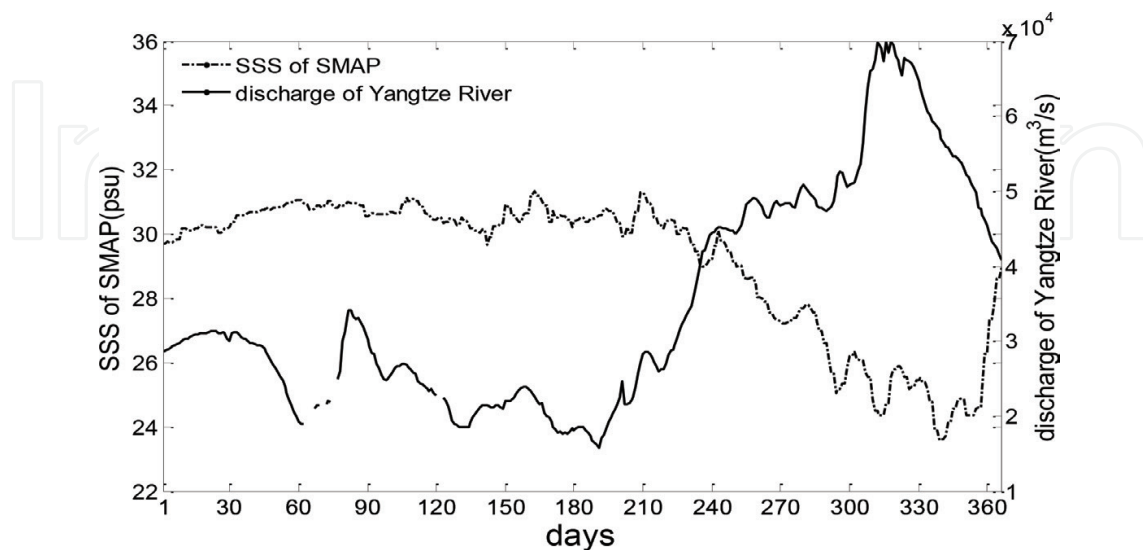


Figure 5. Mean SSS for the region of 32°N to 33°N , 122°E to 124°E from September 2015 to August 2016, representing Yangtze River estuary and discharge of the Yangtze River from the Datong hydrological station during the same period. The unit of salinity is psu. The unit for discharge is m^3/s .

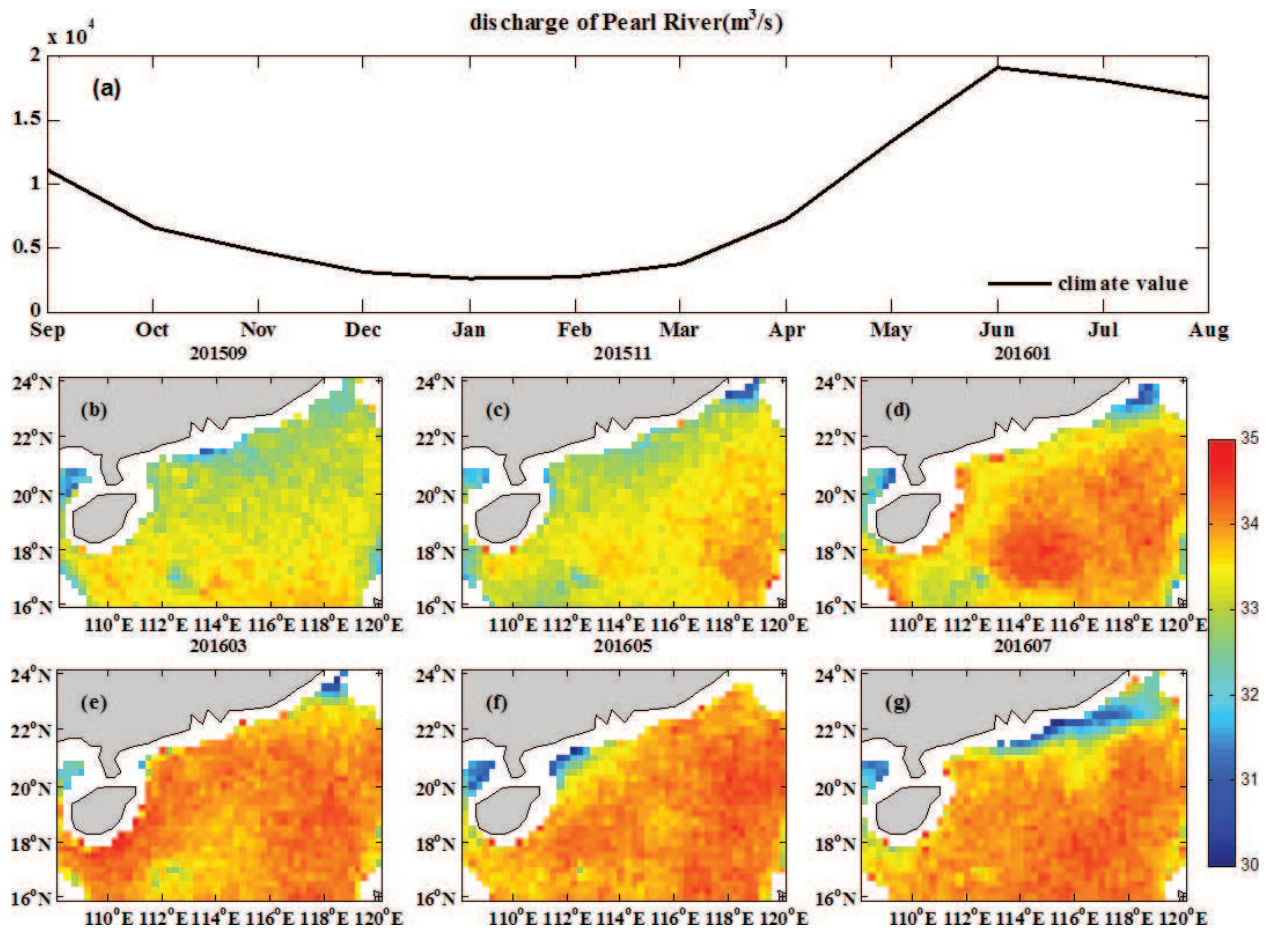


Figure 6. (a) The climate discharge of Pearl River. The distribution monthly SSS from September 2015 to August 2016 over the Pearl River estuary (b)–(g). The unit for SSS is psu. The unit for discharge is m³/s.

freshwater. **Figure 7g–l** shows the distribution of SSS for every 15 days from December of 2015 to February of 2016. We found that the southward diffusion of freshwater plume is weak, the SSS decreasing from 30°N to the South China coastal area and reaching the minimum value. The diffusion is presumably associated with the north wind in winter. Compared with the summer, the scope of the Yangtze River freshwater diffusion is much weaker during winter time.

In addition, **Figure 7g–l** shows that the SSS in the near coastal area 20–34°N, 112–126°E is high at north and south part while low over the Yangtze River estuary. The Yangtze River has a small discharge in winter (**Figure 5**). It flows out of the Yangtze River mouth and spreads to the south near the coastal area and it does not exceed 70 km in the range of 27–31°N. Due to the increasing measurement error of satellite in the near coastal region, the chance of missing data is increased. The diffusion of the Yangtze River freshwater to the south is not as clear as its diffusion to the north. But the phenomenon can be seen from the SMAP data. For example, a low salinity belt can be observed along the coastal area near 30–24°N.

Comparing the diffusion of Yangtze River freshwater in summer and winter, it is obvious that the discharge of Yangtze River is larger in summer than that in winter. The range of diffusion to the northeast direction is far greater than that to the south direction. In addition to the influence of the discharge, the wind is also an important factor. Affected by the monsoon, southerly winds prevail in summer, the Yangtze River discharge flows to the north, while northerly winds reign in winter, and the Yangtze River discharge flows to the south.

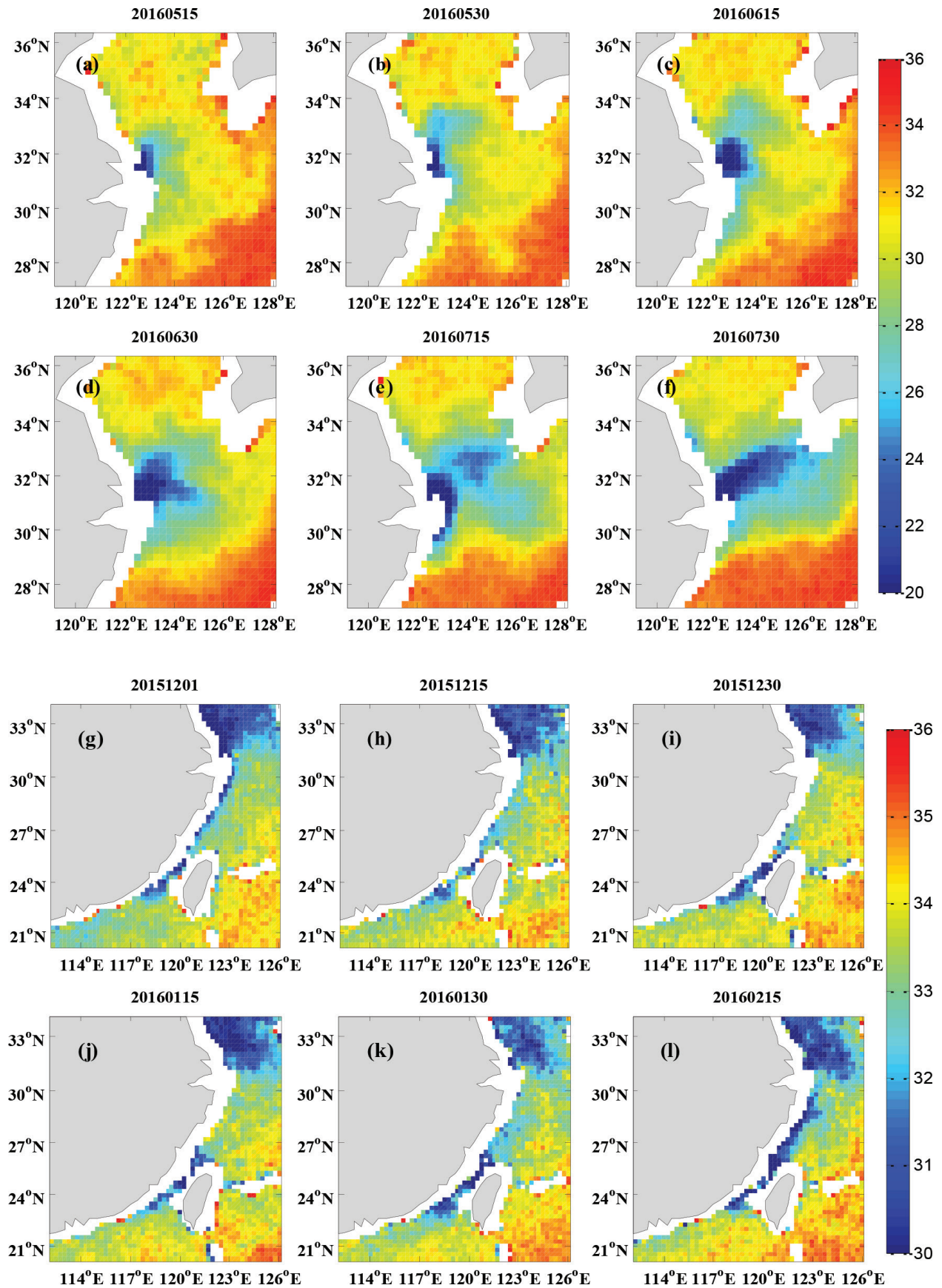


Figure 7. (a)–(f) Daily SSS from May 2016 to July 2016 for every 15 days for the Yangtze River estuary; (g)–(l) same as (a)–(f), but from December 2015 to February 2016. The exact date of the SSS observation is labeled in the top part of each figure. The unit for SSS is psu.

4. Summary

The spatial characteristics and temporal evolution of SSS over the Chinese coastal seas from SMAP data are analyzed in this paper. The results show that the SSS of Chinese coastal seas including the adjacent area of the Yangtze River and Bohai is lower than that of the outer sea. The SSS has obvious seasonal cycle, especially over the Yangtze River estuary. The annual amplitude of SSS change is more than 16 psu with the minimum appearing in summer and the maximum in winter. The SSS over the Pearl River estuary also shows seasonal changes although the change of SSS is relatively small due to the weaker discharge of the Pearl River than that of the Yangtze River. The comparison of SSS from SMAP against in situ observation indicates a RMSD between them is about 3 psu. However, it is encouraging to note that the SSS from SMAP mission can depict the spreading of freshwater plume from the Yangtze River, especially during summer time.

The SSS over Yangtze River estuary is negatively correlated with the discharge. Due to the influence of discharge, the SSS in the Pearl River estuary also shows similar results. However, the SSS difference between summer and winter is smaller than that of Yangtze River estuary. Salinity observation from satellites is an important supplement to in situ salinity observation. It can be used to monitor the diffusion of freshwater discharge in the coastal seas and the real-time prediction of the marine condition.

Acknowledgements

This study was supported by the 2015 Jiangsu Program of Entrepreneurship and Innovation Group, the Ocean Public Welfare Scientific Research Project, State Oceanic Administration of the People's Republic of China (201505003-05), the National Key China (Grant No. 2015g016), and the 2015 Jiangsu Program of Entrepreneurship and Innovation Group (Grant No. 2191061503801/002). Research and Development Program of China (2016YFC1401600) and the Priority Academic Program Development of Jiangsu Higher Education Institutions (PAPD).

Author details

Qiong Wu¹, Xiaochun Wang^{2,3*}, Xianqiang He⁴ and Wenhao Liang²

*Address all correspondence to: xcwang@nuist.edu.cn

1 School of Atmospheric Sciences, Nanjing University of Information Science and Technology, Nanjing, China

2 School of Marine Science/Jiangsu Engineering Technology Research Center for Marine Environment Detection, Nanjing University of Information Science and Technology, Nanjing, China

3 JIFRESSE, University of California at Los Angeles, Los Angeles, USA

4 Second Institute of State Ocean Administration, Hangzhou, China

References

- [1] Bingham FM, Foltz GR, McPhaden MJ. Characteristics of the seasonal cycle of surface layer salinity in the global ocean. *Ocean Science*. 2012;**8**:915-929
- [2] Durack PJ, Wijffels SE. Fifty-year trends in global ocean salinities and their relationship to broad-scale warming. *Journal of Climate*. 2010;**23**:4342-4362
- [3] Bai Y, Pan DL, Cai WJ, He XQ, Wang DF, Tao BY, Zhu QK. Remote sensing of salinity from satellite-derived CDOM in the Changjiang river dominated East China Sea: Satellite salinity of Changjiang plume. *Journal of Geophysical Research: Oceans*. 2013;**118**:227-243
- [4] Bai Y, He XQ, Pan DL, Chen C-TA, Yan K, Chen XY, Cai WJ. Summertime Changjiang river plume variation during 1998-2010. *Journal of Geophysical Research: Oceans*. 2014;**119**:6238-6257
- [5] Subrahmanyam B, Murty VSN, Heffner DM. Sea surface salinity variability in the tropical Indian Ocean. *Remote Sensing of Environment*. 2011;**115**:944-956
- [6] Liu B, Feng L. An observational analysis of the relationship between wind and the expansion of the Changjiang river diluted water during summer. *Atmospheric and Oceanic Science Letters*. 2012;**5**:384-388
- [7] Berger M, Camps A, Font J, Kerr Y, Miller J, Johannessen J, et al. Measuring ocean salinity with ESA's SMOS mission. *ESA Bulletin-European Space Agency*. 2002;**111**:113-121
- [8] Font J, Camps A, Borges A, Martín-Neira M, Boutin J, Reul N, Kerr YH, Hahne A, Mecklenburg S. SMOS: The challenging sea surface salinity measurement from space. *Proceedings of the IEEE*. 2010;**98**:649-665
- [9] Le Vine DM, Lagerloef GSE, Colomb FR, Yueh SH, Pellerano FA. Aquarius: An instrument to monitor sea surface salinity from space. *IEEE Transactions on Geoscience and Remote Sensing*. 2007;**45**:2040-2050
- [10] Lagerloef G, Colomb FR, Le Vine D, Wentz F, Yueh S, Ruf C, et al. The aquarius/SAC-D mission: Designed to meet the salinity remote-sensing challenge. *Oceanography*. 2008;**21**:68-81
- [11] Yueh S, Tang W, Fore A, Hayashi A, Song YT, Lagerloef G. Aquarius geophysical model function and combined active passive algorithm for ocean surface salinity and wind retrieval. *Journal of Geophysical Research: Oceans*. 2014;**119**:5360-5379
- [12] Entekhabi D, Njoku EG, O'Neill PE, Kellogg KH, Crow WT, Edelstein WN, et al. The soil moisture active passive (SMAP) mission. *Proceedings of the IEEE*. 2010;**98**:704-716
- [13] Entekhabi D, Das N, Yueh S, et al. SMAP Handbook Soil Moisture Active Passive: Mapping Soil Moisture and Freeze/Thaw From Space. Instrument Design and L1 Data Products. California, USA: National Aeronautics and Space Administration Jet Propulsion Laboratory, California Institute of Technology Pasadena; 2014. pp. 31-46
- [14] Das NN, Entekhabi D, Njoku EG. An algorithm for merging SMAP radiometer and radar data for high-resolution soil-moisture retrieval. *IEEE Transactions on Geoscience and Remote Sensing*. 2011;**49**:1504-1512

- [15] Yueh S, Fore A, Tang WQ, Hayashi A, Stiles B, Zhang FQ, Weng YH, Reul N. Applications of SMAP data to retrieval of ocean surface wind and salinity. *SPIE Remote Sensing*. 2016;**9999**:99990F
- [16] Fournier S, Reager JT, Lee T, Vazquez-Cuervo J, David CH, Gierach MM. SMAP observes flooding from land to sea: The Texas event of 2015: SMAP observes Texas flooding. *Geophysical Research Letters*. 2016;**43**:10338-10346
- [17] Kim K, Kim KR, Rhee TS, Rho HK, Limeburner R, Beardsley RC. Identification of water masses in the Yellow Sea and the East China Sea by cluster analysis. *Elsevier Oceanography Series*. 1991;**54**:253-267
- [18] Xuan JL, Huang DJ, Zhou F, Zhu XH, Fan XP. The role of wind on the detachment of low salinity water in the Changjiang Estuary in summer: Wind role on the LSW detachment. *Journal of Geophysical Research: Oceans*. 2012;**117**:C10004
- [19] Dai AG, Trenberth KE. Estimates of freshwater discharge from continents: Latitudinal and seasonal variations. *Journal of Hydrometeorology*. 2002;**3**:660-687